ISSN 1069-3513, Izvestiya, Physics of the Solid Earth, 2012, Vol. 48, Nos. 7–8, pp. 653–669. © Pleiades Publishing, Ltd., 2012.
Original Russian Text © D.M. Pechersky, G.P. Markov, V.A. Tsel'movich, Z.V. Sharonova, 2012, published in Fizika Zemli, 2012, Nos. 7–8, pp. 103–120.

Extraterrestrial Magnetic Minerals

D. M. Pechersky, G. P. Markov, V. A. Tsel'movich, and Z. V. Sharonova

Schmidt Institute of Physics of the Earth, Russian Academy of Sciences, ul. Bol'shaya Gruzinskaya 10, Moscow, 123995 Russia

Received November 9, 2011; in final form, February 7, 2012

Abstract—Thermomagnetic and microprobe analyses are carried out and a set of magnetic characteristics are measured for 25 meteorites and 3 tektites from the collections of the Vernadsky Geological Museum of the Russian Academy of Sciences and Museum of Natural History of the North-East Interdisciplinary Science Research Institute, Far Eastern Branch of the Russian Academy of Sciences. It is found that, notwithstanding their type, all the meteorites contain the same magnetic minerals and only differ by concentrations of these minerals. Kamacite with less than 10% nickel is the main magnetic mineral in the studied samples. Pure iron, taenite, and schreibersite are less frequent; nickel, various iron spinels, Fe-Al alloys, etc., are very rare. These minerals are normally absent in the crusts of the Earth and other planets. The studied meteorites are more likely parts of the cores and lower mantles of the meteoritic parent bodies (the planets). Uniformity in the magnetic properties of the meteorites and the types of their thermomagnetic (MT) curves is violated by secondary alterations of the meteorites in the terrestrial environment. The sediments demonstrate the same monotony as the meteorites: kamacite is likely the only extraterrestrial magnetic mineral, which is abundant in sediments and associated with cosmic dust. The compositional similarity of kamacite in iron meteorites and in cosmic dust is due to their common source; the degree of fragmentation of the material of the parent body is the only difference.

DOI: 10.1134/S1069351312070051

INTRODUCTION

Rock magnetic studies are typically conducted for terrestrial objects. However, the Earth is only a small part of the Solar System, which is continually exposed to cosmic influence. Many thousands of tons of extraterrestrial material in the form of meteorites and cosmic dust are annually precipitated to the Earth. Rock magnetic investigations combined with microprobe analysis of this material not only provide information about the cosmic objects, i.e., the sources of extraterrestrial material supplied to the Earth, but also allow elucidating the role and place of the Earth in space.

A great volume of data on the magnetic properties of the rocks has been accumulated recently. These data primarily include the results of thermomagnetic analysis (TMA) at 800°C and microprobe analysis (MPA) of the metallic particles present in the sediments having different ages and deposited in various regions (Pechersky et al., 2008; 2011; Grachev et al., 2009; Pechersky, 2010; Pechersky and Sharonova, 2011; etc.). These studies show that minor concentrations of metallic particles are widespread in the sediments. Typically, concentrations are below 10^{-4}%, very rarely exceeding 10^{-3}%.

Compositionally, the metallic particles in sediments form three groups: (1) pure iron; (2) kamacite with predominantly 5–6% Ni; (3) Fe-Ni alloy with Ni content ranging from 20% up to pure nickel (Fig. 1). The first and the second groups are ubiquitous, which reflects their natural abundance in the cosmic dust. The third group is local and most likely related to the meteoritic falls; probably, it is partially of terrestrial origin. Concentrations of other magnetic minerals of extraterrestrial origin such as taenite and tetrataenite are below 10^{-5}%; schreibersite, troilite, and extraterrestrial pyrrhotite are almost absent in sediments. This fact cannot be accounted for by iron oxidation alone, because kamacite is the most probable candidate to have suffered from secondary oxidation, while this mineral is the major magnetic component of the metallic particles that have survived in the sediments.

By comparing the results of studying metallic particles in the sediments with analogous data for meteorites, we hope to elucidate the correlation between the cosmic dust (and, in particular, the metallic particles

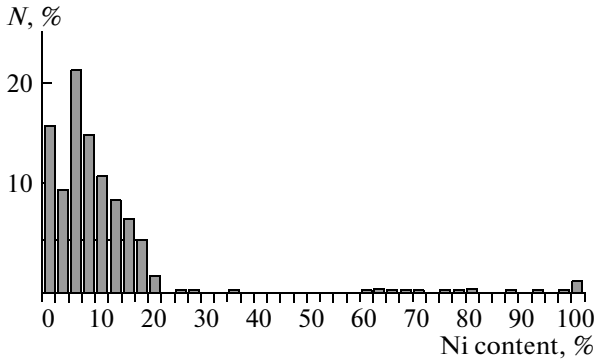

Fig. 1. Histogram of Ni content (%) in the metallic particles from the sediments, according to TMA (Pechersky and Sharonova, 2012).

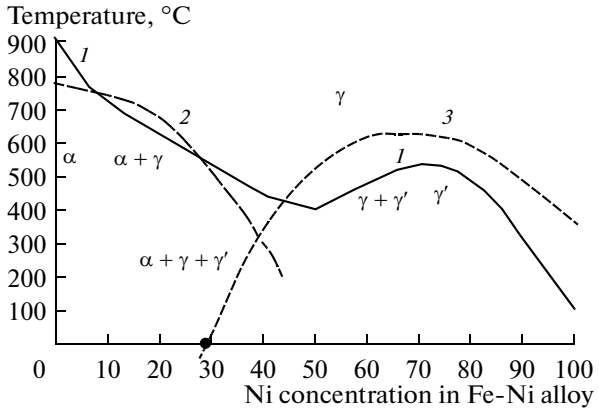

Fig. 2. The phase equilibrium diagram for Fe-Ni alloys (Cassiamani et al., 2006). Line *1* borders the field of stable kamacite (α-phase), taenite (γ-phase), and tetrataenite (γ'-phase). Above line *1* there is taenite only. (*2*) are the Cure points of kamacite; (*3*) are the Curie points of taenite.

in it) and the meteorites. There is also another argument for this research. The analysis of the global data and a set of the reviews (Gus'kova, 1972; Kohout, 2009; Rochette et al., 2009; Terho et al., 1993; Weiss et al., 2009; etc.) shows that previous investigations of the magnetic properties of the meteorites addressed a rather limited range of issues. They included (1) measuring magnetic susceptibility; (2) assessing the origin of natural remanent magnetization and paleointensity at the time of formation of parent cosmic bodies; (3) measuring the magnetic properties of separate meteorites (the granules from chondrites); and (4) analyzing magnetic signatures of tetrataenite, the role of deformations, impact remanent magnetization, etc. (Nagata, Funaki, and Danon, 1986; 1987; Rochette et al., 2009; Sugiura and Strangway, 1981; 1987; Uehara and Nakamura, 2006; Wasilewski, 1988; etc.). However, magnetomineralogical generalizations based on the results from TMA, MPA, and other types of material analyses have not been conducted to date.

In the present paper, we study magnetic properties of extraterrestrial samples by TMA up to 800°C combined with MPA in order to identify common features of the meteorites.

A REVIEW ON THE MAGNETIC MINERALS OF THE METEORITES

According to the Meteoritical Bulletin (2000–2010), meteorites contain the following magnetic minerals.

1. Fe-Ni alloys: kamacite, an alloy with low Ni content typically ranging within 5–6%; taenite, most frequently containing 20–30% and, far less frequently, 40% Ni; and awaruite, where Ni makes up more than 60%. Taenite is mentioned less often by a factor of 2–3 in the Meteoritical Bulletin than kamacite; kamacite's predominance over taenite is also supported by the average Ni content in the iron meteorites (8.81 ± 3.48%). Awaruite is documented in only three cases. Kamacite (α-phase) has an ordered body-centered cubic matrix; taenite and awaruite (γ-phase) have a disordered face-centered cubic matrix, and tetrataenite (γ'-phase) has an ordered face-centered cubic matrix. The iron-nickel phase diagram (Fig. 2) shows that, depending on the Ni content and temperature, the kamacite-taenite-tetrataenite system is present below the black line, whereas above it there is only taenite. In a temperature interval about the Curie point (T_c) of kamacite and taenite, structural transformation $\alpha \leftrightarrow \gamma$ takes place, whose temperature can easily be confused with T_c. In most cases, kamacite contains at most 10% Ni, and with this composition, structural transformation of kamacite to taenite occurs above T_c of kamacite. Therefore, the TMA of the meteorites typically records T_c of kamacite.

The phase diagram (Fig. 2) also shows that taenite with less than 30% Ni has negative T_c (i.e., room temperature and below), and this type of taenite at a higher temperature is paramagnetic. Therefore, in alloys with 0 to 30%Ni, the value $T_c > 500$°C revealed for the meteorite exclusively refers to kamacite. In turn, T_c of kamacite with more than 50% Ni is below room temperature, i.e., in this interval of concentrations, TMA should detect taenite only. We note that there is a magnetic clue as to the difference between tetrataenite and taenite (Nagata, Funaki, and Danon, 1986; 1987): the coercive force of tetrataenite is several orders of magnitude higher than that of taenite. Therefore the coercive force (H_c), remanent coercive force (H_{cr}), and the remanent saturation magnetization ratio to the saturation magnetization (M_{rs}/M_s) abruptly drop at irreversible phase transformation tetrataenite → taenite. The flat shape of the $M(T)$ curve up to 500–700°C is characteristic for tetrataenite, while its sharp decrease above 700°C is a signature of the structural transformation of kamacite to taenite (Nagata, Funaki, and Danon, 1986; 1987; Wasilewski, 1988). Specific saturation magnetization of the Fe-Ni alloy containing less than 20% Ni is almost constant ($M_s = 217.75$ Am^2/kg at room temperature). When Ni content exceeds 20%, this dependence is close to linear. Pure nickel has $M_s = 56.7$ Am^2/kg (Bozorth, 1951).

We also mention another important fact, which is always observed in TMA of Fe-Ni alloys: the temperature of taenite → kamacite transformation ($T_{\gamma \to \alpha}$) during the cooling of the sample lags the temperature of kamacite → taenite transformation ($T_{\alpha \to \gamma}$) during its heating. This temperature lag emerges because the boundaries of the phase fields in the iron-nickel phase diagram can only be determined if the cooling rate does not exceed ~10°C per day (Bozorth, 1951). The shift of the $M(T)$ curves during the heating–cooling cycle unambiguously points to the presence of a Fe-Ni alloy in the sample.

2. Schreibersite $(Fe, Ni)_3P$ is a ferromagnetic mineral with 5–50% Ni. The magnetic properties of native schreibersite are obscure. Artificial Fe-Ni phosphides demonstrate almost linear M_s and T_c dependences on the nickel content (Meyer and Cadeville, 1962; Gambino, McGuire, and Nakamura, 1967).

3. Cohenite $(Fe, Ni)_3C$ is a ferromagnetic mineral that rarely occurs in meteorites (only two occurrences documented). The magnetic properties of cohenite are very poorly known. The artificial analog of cohenite, cementite, has $T_c = 210°C$ and $M_s = 128$ Am^2/kg.

4. Fe-sulfides. Magnetic minerals of this group identified in the meteorites are largely dominated by troilite (FeS), which is an antiferromagnetic with very low magnetization. Besides troilite, pyrrhotite (FeS_{1+x}), pentlandite $(Fe, Ni)_9S_8$, daubreelite ($FeCr_2S_4$), and other sulfides are common. Among these varieties, the monocline pyrrhotite ($0.1 < x < 0.25$) is the only ferrimagnetic mineral with $M_s = 16$ Am^2/kg and $T_c = 325$–$360°C$. Hexagonal pyrrhotite is antiferromagnetic ($0 < x < 0.1$) with $M_s \le 0.1$ Am^2/kg and $T_c = 325°C$. We note that Fe-sulfides are a potential source of magnetite, which is formed as a product of their oxidation in the near-Earth and terrestrial environment.

5. Magnetite (Fe_3O_4) is a ferrimagnetic mineral widespread in terrestrial rocks. According to the published data, magnetite in the meteorites is more frequently formed through secondary alterations on Fe-Ni alloy, schreibersite, and Fe-sulfides; however, it also occurs in the meteorites as an independent species. Magnetite is scarcely reported for iron meteorites and is documented for 8% of stony meteorites. Magnetite predominance in stony meteorites in contrast to iron meteorites is due to the fact that minerals of the magnetite group relate to crustal meteorites (by analogy with the terrestrial conditions), while the remaining meteorites containing Fe-Ni alloy are most likely to have originated from the core and the lower mantle of meteoritic parent bodies.

Terrestrial magmatic mafic rocks (basalts) provide suitable conditions for the crystallization of ferrospinels, which are dominated by titanomagnetite varieties ranging from uniform species with 12–14% titanium to those close to magnetite (Pechersky et al., 1975; Pechersky and Didenko, 1995). This is also valid for crustal meteorites from the Moon and Mars. Direct testing of the lunar basalts delivered to the Earth and the lunar meteorites collected on the Earth's surface (Frondel, 1975; *Meteoritical...*, 2000–2010) revealed chromite, ulvospinel, and their solid solutions, ilmenite, Fe-sulfides (mainly pyrrhotite and trolilte), and minor concentrations of pure iron. According to (*Meteoritical...*, 2000–2010), Martian basalt meteorites contain titanomagnetite and ulvospinel, chromite (frequently with titanium, aluminum, and magnesium admixtures), ilmenite, and Fe-sulfides, mainly pyrrhotite and troilite. Kamacite and taenite of probably impact origin are very rare.

Quite different conditions are observed in the mantle. The measurements of the magnetic properties of the rock samples from the upper mantle (mantle xenoliths from flood basalts and peridotites from suboceanic mantle) indicate that primary magnetic minerals of magnetite group are absent there (*Petromagnitnaya...*, 1994).

6. Ilmenite ($FeTiO_3$) is paramagnetic at room temperature. It is the endmember of the solid solution series of ilmenite–geikielite–pyrophanite and other, in particular, hemoilmenite ($Fe_{2-x}Ti_xO_3$). At $x = 0.9$–0.4, hemoilmenite is ferrimagnetic with M_s up to 60 Am^2/kg (Nagata, 1961). The meteorites only contain ilmenite (with x about 1) with minor concentrations of magnesium, i.e., paramagnetic mineral.

THE COMPOSITION AND MAGNETIC PROPERTIES OF THE METEORITES AND TEKTITES

The Samples and Experimental Procedure

The studied meteorite samples (40 samples of 25 meteorites) and 3 tektite samples were selected from the collections of the Vernadsky Geological Museum of the Russian Academy of Sciences (Moscow) and the Museum of Natural History of the North-East Interdisciplinary Science Research Institute, Far Eastern Branch of the Russian Academy of Sciences (Magadan) (Table 1). These meteorites were collected from very diverse regions of the Earth; their falls cover a time span of at least three centuries; therefore, the studied set of the samples is sufficiently representative for revealing general trends in the distribution, composition, and magnetic properties of the magnetic minerals contained in the meteorites.

The meteorites and tektites were studied by a complex of methods including magnetic measurements, TMA, and MPA. Remanent magnetization of the samples was measured by the JR-6 spinner magnetometer manufactured by AGICO (Czech Republic). The sensitivity of the instrument is 2×10^{-11} Am^2. The coercive force and remanent coercive force were measured by the Variable Field Translation Balance (Petersen Instruments, Germany). TMA and saturation magnetization measurements were conducted using the thermovibrational magnetometer designed by N.M. Anosov and Yu.K. Vinogradov (Institute of Physics of the Earth, Russian Academy of Sciences), which has a sensitivity of 10^{-8} Am^2. During TMA, the magnetization M of the sample exposed to a constant magnetic field of 600 mT was continually measured during heating the sample to 800°C and its subsequent cooling to room temperature. Normally, the heating–cooling cycle was repeated twice.

Table 1. The results of thermomagnetic and microprobe analyses of meteorite and tektite samples

Meteorite, country	Sample	M_s	M_{rs}/M_s	M_{st}/M_s	H_{cr}	H_{cr}/H_c	H_{crt}/H_{cr}	Kamacite			Schreibersite			$T\gamma \rightarrow \alpha$	Taenite			Other minerals
								T_c	Nit	Nip	T_c	Nit	Nip		T_c	Nit	Nip	
1	2	3	4	5	6	7	8	9	10	11	12	13	14	15	16	17	18	19
Avgustinovka, octahedrite, Ukraine	Gr7366	6.3	0.19	1.0	15	1.6	1.38	720; 740	12; 7	3.6?	nd	nd	nd	?	nd	nd	nd	secondary oxides
		5.8	0.26		15		3.00											
	Gr7363	6.9	0.26	1.8	22.5		2.09	720; 750	12; 5	2.3?	nd	nd	nd	?	nd	nd	nd	secondary oxides,
		1.8			22		2.14											sg Fe-Ni-Cr, Fe-Cr-Al, and Fe-Cu-Zn alloy;
	Gr7364	7.7	0.28	0.9	29.0		1.79	720; 740	12;7	3.6?	nd	nd	nd	?	nd	nd	nd	secondary oxides
Aliskerovo, octahedrite, NE Russia	AL-1	154.5	0.01	0.9	10		2.3	I-764	2.5	6.8	nd		sg	630	nd	nd	sg14–17	aluminosilicates;
								II-744	6.3	6.8								secondary oxides
Anui, hexahedrite, NE Russia	AN-1	128.6																aluminosilicates, sg troilite, chromite, daubreelite, and lead
Babbs Mill, octahedrite, USA	Gr7389	143.3	0.01	0.26	25		1.48	738	7.7	6.6	nd		sg	620	nd	nd	sg19.6	secondary oxides,
								600										abundant magnetite
Bilibino, octahedrite–hexahedrite, NE Russia	BIL-1	132.9	0.025	1.0	7.0		0.74	I-770	0	4.7	nd		sg 16–21.6	665	nd	nd	nd	aluminosilicates;
								II-757	3.2	4.7				657				secondary oxides
Bishtyube, octahedrite, Kazakhstan	Gr7369	4.7	0.19	0.2	10.9	9.9		770. 753	0; 4	0; 6.5	nd	nd	nd	–	nd	nd	sg75.7	Hg-Fe-Cu sulfides,
								II-595			nd	nd	nd		nd	nd	nd	sg lead, secondary oxides
	Gr7370	48.4	0.003	1.0	36.0													secondary oxides
Grossliebental, chondrite, Ukraine	Gr7373	1.13	0.02	0.95	80.0	5.2	0.15	730	9.7	14.3	nd	nd	nd	650	nd	nd	21-46	olivine, pyroxene,
								630	17	14.3				200?				troilite, pyrrhotite,
		1.49																pentlandite, chromite, secondary oxides, cinnabar
Gibeon, octahedrite, Namibia	Gr7404	175.0	0.009	0.93	11		1.0	I-747			nd	nd		634	nd	nd		
								II-739	7.5					650				

Table 1. (Contd.)

Meteorite, country	Sample	M_s	M_{rs}/M_s	M_{st}/M_s	H_{cr}	H_{cr}/H_c	H_{crt}/H_{cr}	Kamacite			Schreibersite			$T\gamma \rightarrow \alpha$	Taenite			Other minerals
								T_c	Nit	Nip	T_c	Nit	Nip		T_c	Nit	Nip	
1	2	3	4	5	6	7	8	9	10	11	12	13	14	15	16	17	18	19
Zabrod'e, chondrite, Belorussia	Gr7445	4.0	0.03	0.62	17.1	5.4	1.99	I-750 II-734	4.9	5.4	nd	nd	nd	625	nd	nd	17–48	olivine, pyroxene, troilite
Imilak, pallasite, Chile	Gr7409	95.9	0.004	1.0	1.1	8.8	1.5	I-757 II-734	3.0 8.7	5.6	nd	nd	nd	642 620	nd	nd	nd	aluminosilicates, olivine, sg ilmenite secondary oxides
Cumberland Falls, achondrite, USA	Gr7441	10.87	0.004	0.91	22.5		1.5	762; 630	2.0	5.7	nd	nd	22.3	655	nd	nd	42.8 22.7	olivine, sg nickel, troilite, pentlandite, pyrrhotite, cinnabar
Cosby's Creek octahedrite, USA	Gr7430	53.9 0.12	0.25 0.21	1.0	24.6 26.0	2	2.0	I-635; 720 II-606; 745	720 6.0	0–6.8 0–6.8			sg 34	– 630	nd	nd	sg 31	secondary wustite, magnetite, and other oxides
Krasnoyarsk, pallasite, Russia	Gr7374	148.3	0.001	1.0	14.6	24.3		734	8.7	5.4	nd		28.3	620	nd	nd	nd	aluminosilicates, pentlandite, pyrrhotite, cinnabar sg lead, antimony, cassiterite, and ilmenite; secondary oxides
Krasnoyarsk, olivine separate	Gr7375	0.7	0.16	1.0	26.5	2.1	1.62	nd	nd	nd	150	32	29	–	nd	nd	nd	I-III-285 – Fe-oxide; olivine, sg troilite and cinnabar secondary oxides
Krasnoyarsk, magnetic fraction from olivine separate	Gr7375m	16.9	0.26	0.87				750	4.9		168	29.5	29	662	nd	nd	nd	secondary magnetite $T_c = 600°C$ (2%); olivine; secondary oxides
Krasnoyarsk, low-magnetic fraction	Gr7375sh	0.7		4.0					nd	nd					nd	nd	nd	Fe-oxide with S and Ni (30%M_s), magnetite
Krasnoyarsk, pallasite, Russia	mn29874	123.9	0.002	0.98	17		1.76	750	4.9	4.8	nd	nd	27.9	620 250?	nd	nd	nd	olivine; sg troilite, corundum, and cinnabar; secondary oxides
Marjalahti, pallasite, Russia	Gr6490	172.8	0.001	0.98	15	150	1.13	759	2.7	3.0	nd	nd	sg 56.6	640	nd	nd	sg 26; 54	silicates Fe-Al alloy
Omolon, pallasite, CB Russia	OM-1	102.0	0.008	0.9	17		1.59	I-762 II-744	2.0 6.3	 5.6	210	24	23.8	I-725; 644 II-725; 658	nd	nd	27–48	olivine, secondary oxides

Table 1. (Contd.)

Meteorite, country	Sample	M_s	M_{rs}/M_s	M_{st}/M_s	H_{cr}	H_{cr}/H_c	H_{crt}/H_{cr}	Kamacite			Schreibersite			$T\gamma \rightarrow \alpha$	Taenite			Other minerals
								T_c	Nit	Nip	T_c	Nit	Nip		T_c	Nit	Nip	
1	2	3	4	5	6	7	8	9	10	11	12	13	14	15	16	17	18	19
Omolon,	Gr0010a	147.8	0.003	1.0	14.5		0.9	760	2.5	4.6	nd	nd	nd	649	nd	nd	nd	secondary oxides
pallasite, CB Russia	Gr0010c	149.4			11.5		1.09	nd	nd	4.1	nd	nd	24		nd	nd	nd	
Okhansk, chondrite, Russia	Gr7387	20.7	0.13	0.98	46		0.76	734	8.7	5.6	nd	nd	nd	640	560	53	45.3	olivine, troilite, pyrrhotite, sg Cu-Fe-sulfides
Santa Catarina,	Gr7362	6.62	0.056	0.95	16	2.29		I-747	5.6	0.2–4.6	nd	nd	nd	630	nd	nd	nd	secondary oxides
iron, Brazil		0.2	0.12	0.78	12		2.25	II-750	4.9	0.2–4.6				605				
Sao Juliao de Moreira	Gr7428	113.1	0.003	0.9	11.5	20.4	1.09	I-nd II-nd	nd	5.7	I-335 II-325	12 13	11.6 13	?	nd nd	nd nd	nd nd	secondary oxides Fe-Al alloy, corundum,
hexaoctahedrite	Gr7427	105.7	0.001	0.97	15		1.60	760	2.4	4.8			nd	670	nd	nd	nd	hercynite,
Portugal								758	3.0	4.8				668	nd	nd	nd	secondary oxides
Saratov, chondrite, Russia	Gr7379	17.7	0.016		75		1.12											
″	Gr7380	16.1	0.014	0.98	75.8	27.4		I-765 II-755 III-752	1.0 3.6 4.4	0 3.3	nd	nd	nd	?	I-630	65		
″	Gr7381	16.3	0.015	0.97	164	24.5		I-750 I-750	4.9 4.9		nd	nd	nd	?	I-615 II-580	65 55		
″ MPA data generalization	Gr7379-7380-7381-7383									0 3.3	nd	nd	nd		nd	nd	20.7 47.1	olivine, pyroxene, troilite, pyrrhotite, pentlandite, aluminosilicates; sg Fe-chromide, Cr-Fe spinels, daubreelite, copper, cinnabar, and nickel
Seimchan, octahedrite CB Russia	SM-1	95.8	0.016	0.77	9.0		1.78	I-762 II-745	2.0 6.1	8.7 8.7	nd		25.8	670	nd	nd	11–21	olivine, pyroxene; secondary oxides
Sikhote-Alin,	Gr7439	137.4	0.003	1.0	26.5		1.28	I-767	0.7	5.7	nd	nd	nd	650	nd		sg16;	olivine, pyroxene,
hexaoctahedrite,								II-752	4.4	5.7							49.6	aluminosilicates;
Russia	Gr7439a	153.5		0.97				767	0.7	5.7	nd			635	nd	nd	nd	sg troilite and pentlandite, Aluminum iron spineles, carbonates, secondary oxides

Table 1. (Contd.)

Meteorite, country	Sample	M_s	M_{rs}/M_s	M_{st}/M_s	H_{cr}	H_{cr}/H_c	H_{crt}/H_{cr}	Kamacite			Schreibersite			$T\gamma \rightarrow \alpha$	Taenite			Other minerals
								T_c	Nit	Nip	T_c	Nit	Nip		T_c	Nit	Nip	
1	2	3	4	5	6	7	8	9	10	11	12	13	14	15	16	17	18	19
Tektites moldavite; Czechia	Gr7601,	0.026	0.12	?	25.5		1.08	nd	nd	nd	nd	nd	nd		nd	nd	nd	
indochinite	7604-1,	0.017										nd	nd				nd	aluminosilicate
indochinite	7604-2	0.386						745	6	nd	nd	nd	nd		nd	nd	nd	glass
Vietnam	gr7605	0.074						720?	12?	nd	nd	nd	nd		nd	nd	nd	magnetite, 0.02–0.08%
Toluca,	Gr7436	100.9	0.008	0.95	12		1.17	I-750	4.9	6.4	nd	nd	nd	602	nd	nd	nd	secondary
octahedrite,								II-743	6.6	6.4				603				Foxides
Mexico	gr7437	101.1	0.002	1.01	13		1.83	I-751 II-742	4.6 6.8	6.4 6.4			sg 34	620 620	nd	nd	nd	
Hainholz mesosiderite Germany	Gr7405	0.56	0.12		53.7	9.7				5.8			nd	?			46.3; 65.7	silicates, Cr-Fe spinels, oxides
Hassle,	Gr7406	4.9	0.062	1.06	76.0	18.1	0.37	760;	2.5	0.6	nd	nd	nd	670	nd	nd	52.8	olivine, pyroxene;
chondrite, Sweden								680	17	15.0				60 2				sg nickel; troilite, pyrrhotite; oxides
Egvekinot,	EGV-1	84.4	0.034	0.95	62.0		0.36	I-761;	2.5	10	nd	nd	sg 38	585	?	?	sg 19–52	silicates; trevorite,
octahedrite								650	15	10				265				chromium;
CB Russia								II-738;	7.8	10				585				oxides
								650	15	10				265				

Notes: The Meteorite column contains the name of the meteorite, its type, and the country of finding. The Sample column contains the code of the sample in the museum collection. M_s is specific saturation magnetization of a sample before heating, Am^2/kg; M_{rs} is specific remanent saturation magnetization; M_{st} is specific saturation magnetization measured after heating a sample to 800°C; H_{cr} is the remanent coercive force measured before heating, mT; H_c is coercive force, mT; H_{crt} is remanent coercive force measured after heating a sample to 800°C. In the columns entitled "kamacite," "schreibersite," and "taenite," T_c is the Curie point, °C; I and II are the first and the second heatings; Nit and Nip is Ni content in a given mineral measured by TMA and MPA, respectively; $T\gamma \rightarrow \alpha$ is the temperature of transformation of taenite to kamacite upon cooling of the sample, °C; sg means single grains; nd means that the mineral is not detected.

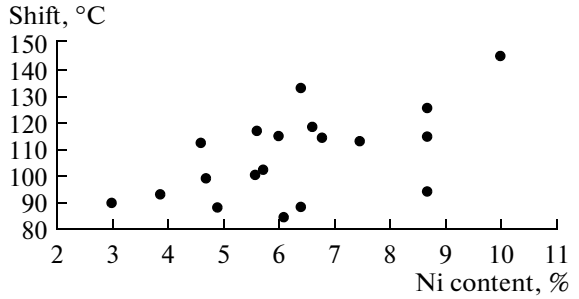

Fig. 3. The shift of the temperature of taenite → kamacite structural transformation relative to the Curie point of kamacite upon cooling the sample (mainly according to the results for the second heating, when the measured Curie point approaches the theoretically predicted value). The horizontal axes measures the average Ni content in kamacite (%) determined by the microprobe; the vertical axis measures the temperature shift, °C.

For estimating the concentration of the magnetic mineral in the sample, the $M(T)$ curve was extrapolated from each Curie point to room temperature. Then, the M_s for the mineral with a given Curie point was determined. The ratio of the obtained M_s to the known saturation magnetization of the given mineral provides the content of the studied mineral in the sample.

Microprobe measurements were conducted by the TESCAN Vega II scanning electron microprobe integrated with an energy dispersive X-ray micro-analyzer. The micrograins were initially examined under the microscope and then subjected to MPA. The optical microscopy measurements were carried out by the Olympus BX51M microscope. The photos from optical microscope were processed by the Combine ZP program designed by Alan Hadley. This software blends partially focused individual 3D microscopic images into a composite photo and thereby increases the depth of the focus. The grains selected for the analyses were stuck on a double-layer electrically conductive carbon adhesive tape and then squeegeed by a glass rod in order to make the surface of the particles parallel to the surface of the objective table. This allowed us to analyze the particles without polishing thin sections of specimens, which would have resulted in additional contamination of the object and a loss of some particles. The microprobe measurements were conducted with an accelerating voltage of 20 kV and a beam current of 0.2 nA. The diameter of the probe was ~2 μm.

The Results of the Study of Magnetic Minerals in Meteorites

The results are summarized in Table 1 and in the *Supplement*.[1]

[1] Accessible at http://paleomag.ifz.ru/books/2012-pechersky-et-al-meteorite-data-supplement.rar.

Kamacite. Among all magnetic minerals identified and analyzed by MPA, TMA most distinctly distinguishes kamacite in all the studied meteorites (except Bishtyube meteorite, which only contains pure iron). Kamacite is recognized by two features: (a) T_c is present in the heating curve, since $T\alpha \rightarrow \gamma$ is higher than or close to T_c if kamacite contains up to 10% Ni (Fig. 2) and (b) $T\gamma \rightarrow \alpha$, which is shifted by about 100°C from T_c, is identified during cooling the sample to 800°C (Bozorth, 1951). Although this shift noticeably varies due to a variety of factors, it generally tends to increase with increasing Ni content in kamacite (Fig. 3).

Taenite with nickel content typically exceeding 30% is revealed by MPA in 12 samples; it is not rare for it to occur as single grains undetectable by TMA (Table 1; Pechersky et al., 2011a). TMA reveals taenite in only three samples (Okhansk, Saratov, and Egvekinot). Among the samples containing taenite, four are iron meteorites, two are stony-iron meteorites, and six are stony meteorites, i.e. all the studied samples of stony meteorites contain taenite. Here, kamacite and taenite never compose a continuous series of solid solutions but rather crystallize separately (segregated). For example, the samples from the Grossliebental, Zabrod'e, Okhansk, Saratov, Hainholz, and Egvekinot meteorite contain isolated large grains and segments of kamacite intergrown with taenite, which are distinctly seen when scanned under the microscope, e.g., in the Saratov chondrite (Fig. 4). The separate segregated crystallization of the three main magnetic minerals (kamacite, taenite, and schreibersite) is accentuated by the absence of a correlation between the concentrations of these minerals: the coefficients of linear correlation between the contents of kamacite and taenite R_{kt}, kamacite and schreibersite R_{ks}, and taenite and schreibersite R_{ts} are −0.082, −0.087, and −0.073, respectively.

Besides isolated intergrowths of kamacite and taenite, thin lamellae of taenite in kamacite are also common. These were formed as a result of kamacite decomposition (Nagata, Funaki, and Danon, 1986; Nagata, Danon, and Funaki, 1987). Typically, taenite lamellae are thinner than the diameter of the probe and are only recognizable by a somewhat increased Ni content; in this case, the average composition of kamacite is estimated by MPA. The decrease in the Curie points of kamacite after heating the samples to 800°C is a thermomagnetic signature of the existence of these structures. This trend is clearly pronounced in Fig. 5. Upon the first heating, the Curie points in most cases do not depend on the Ni content and are very close to T_c of pure iron; i.e., kamacite is represented by thin lamellae of taenite in almost pure iron in most of the studied meteorites. The second heating causes homogenization of the solid solution; T_c decreases and becomes dependent on the nickel concentration in kamacite.

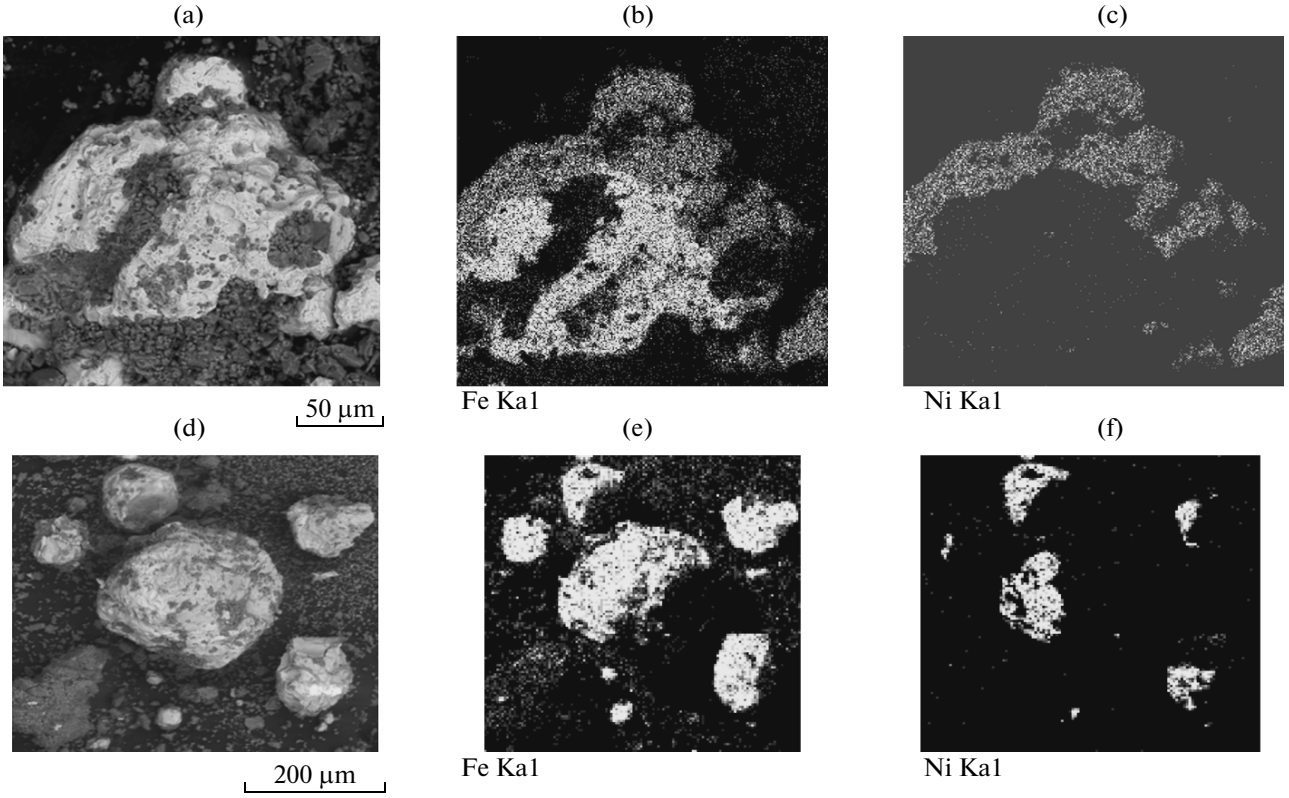

Fig. 4. (a), (d) The grains composed of taenite and kamacite. The contours of both minerals are seen in the scans for ((b) and (e)) iron and ((c) and (f)) nickel. The Saratov meteorite.

Schreibersite is distinctly distinguished by TMA by its Curie point; the Ni content in schreibersite is consistent with the empirical dependency for artificial Fe-Ni phosphides (Meyer and Cadeville, 1962; Gambino, McGuire, and Nakamura, 1967). The microprobe recognized schreibersite in 40% of the samples; however, its high concentrations are revealed by both MPA and TMA only in three meteorites (Krasnoyarsk, Omolon, and Sao Juliao de Moreira). MPA detected single schreibersite grains in another 9 meteorites (Anyui, Avgustinovka, Bilibino, Cumberland Falls, Cosby's Creek, Seimchan, Sikhote-Alin, Toluca, and Egvekinot). However, TMA did not recognize these grains; i.e., they contribute far below 1% to M_s. Neither MPA nor TMA revealed schreibersite in the remaining 13 meteorites.

Where identified, schreibersite is highly nonuniformly distributed in a meteorite. For example, in the Krasnoyarsk meteorite, schreibersite is only abundant in sample gr7375, whereas samples gr7374 and MH29874 only contain single schreibersite grains. A high concentration of schreibersite is found in the OM-1 sample from the Omolon meteorite; its single grains are detected in sample gr0010v, while sample gr0010a does not contain schreibersite altogether. Sample gr7428 from the Sao Juliao de Moreira meteorite is characterized by a high concentration of schreibersite, although schreibersite is not identified in sample gr7427 from this meteorite (Pechersky et al., 2011a). Schreibersite contains 8 to 66% Ni (Marjalahti); the average Ni concentration in schreibersite on its contact with kamacite and taenite is 20 and 30%, respectively.

Cohenite has neither been detected by TMA nor by MPA in the studied samples.

Nickel. Single nickel grains are identified by MPA in the Saratov, Hessle, and Cumberland Falls meteorites; however, they are not detected by TMA; i.e., their contribution to M_s is far below 1%.

Fe-Al Alloy. Grains of the Fe-Al alloy that are uncommon for meteorites are recognized in the form of inclusions in kamacite in the Marjalahti and Sao Juliao de Moreira meteorites (Fig. 6). The Fe-Al alloy has the following average composition: 4.1% O; 4.6% Al; 89.9% Fe ($n = 13$) (Marjalahti) and 2.5% O; 6.2% Al; 78.1% Fe; and 0.2% Ni; ($n = 6$) (Sao Juliao de Moreira). Spots with increased concentrations of aluminum (9.7% O; 16.7% Al; 57.9% Fe; 1.6% Ni; $n = 5$) and carbon (6.3% O; 17.1% Al; 21.5% Fe; 55% Ni; $n = 5$) gravitate to the marginal parts of the second sample. We note that artificial Fe-Al alloys are common (e.g., alfer and alphenol).

Fe-oxide with sulphur and nickel admixtures. Fe-oxide with some amounts of sulphur and nickel is

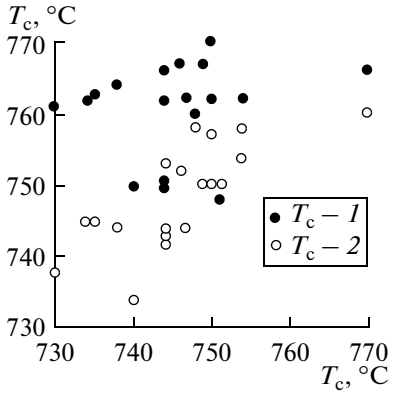

Fig. 5. The displacement of the measured Curie points towards the theoretical predictions after heating the meteoritic samples to 800°C: (*1*) the first heating; (*2*) the second heating.

identified in a low-magnetic fraction of sample gr7375sh from the Krasnoyarsk meteorite (Fig. 7). The average composition of this magnetic mineral is 44.3 % O; 2.4% S; 47.5% Fe; and 4.3% Ni. Sulfur content slightly varies from 1.8 to 2.8%. The concentration of nickel ranges from 2 to 7%, probably depending on the composition of kamacite after which this mineral is formed. This mineral crystallizes in various forms; for example, it makes crusts on other minerals (Fig. 7a) or appears as filaments (Fig. 7b). Evidently, this mineral only contains Fe^{3+}; therefore, it is stable on heating. Its Curie point ($T_c = 280–290$°C) is close to the Curie point of magnesioferrite and jacobsite. The $M(T)$ curves for cooling and heating (Fig. 8) reflect only two magnetic phases: the Fe-oxide with a sulfur and nickel admixture, and $T_c = 280$°C, which is of interest for our analysis, and magnetite. Using these data, we can estimate specific saturation magnetization of Fe-oxide containing sulfur and nickel. The total $M_s = 3.17$ AM^2/kg (when heated to 800°C, the initial $M_s = 0.69$ Am^2/kg has increased by a factor of 4.6). Magnetite makes up 79% of this value (Fig. 8), or 2.5 Am^2/kg; the magnetite content in the sample is $2.5/92 = 2.7\%$, and the remaining 97.3% is due to the phase with $T_c = 280$°C (Fig. 8). Thus, M_s of this phase is $(3.17 - 2.5)/0.973 \approx 0.69$ Am^2/kg, which coincides with the initial M_s of the sample; i.e., the initial magnetic material in this fraction is solely Fe-oxide with sulfur and nickel admixtures.

The MPA of all the studied samples revealed small concentrations of these Fe-oxides with sulfur and nickel admixtures in Avgustinovka, Bishtyube, Grossliebental, Zabrod'e, and Cosby's Creek; they only occur within substantially altered segments of the meteorites.

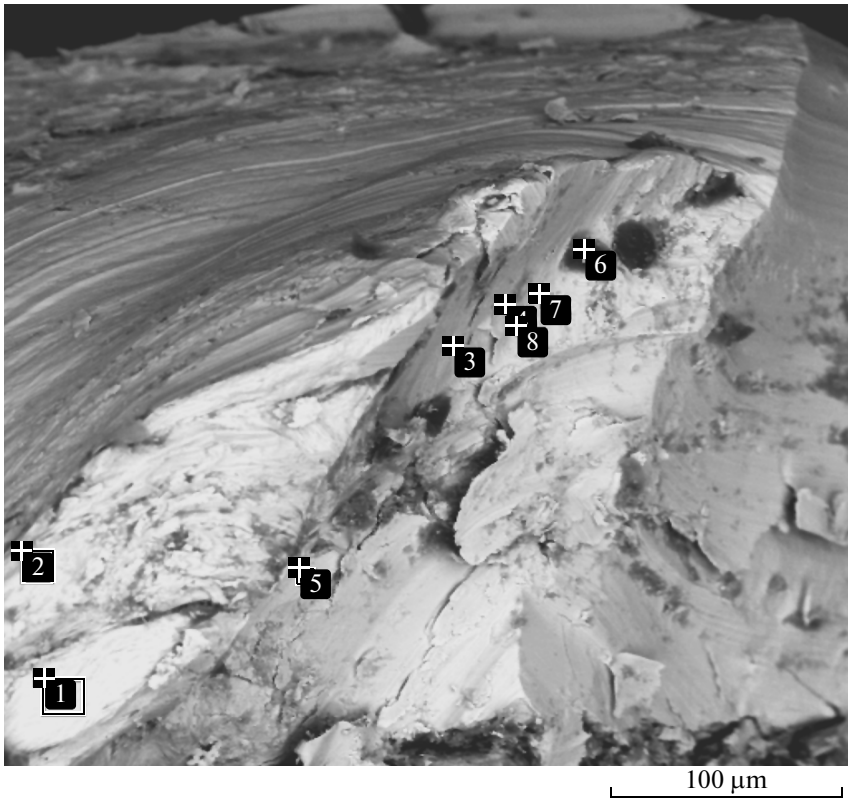

	C	Al	Fe	Ni
1			97.08	
2			94.26	2.92
3		65.73	34.27	5.74
4		34.23	65.77	
5		66.96	33.04	
6	61.27	14.90	23.83	
7		4.53	95.47	
8		13.76	86.24	

Fig. 6. The example of Fe-Al alloy (3–8) in kamacite (1, 2) (Sao Juliao de Moreira, gr7427). The Al-rich segments gravitate to the margins of Fe-Al alloy (3, 5). The black spots are carbon-rich areas (6); the phases are small and heterogeneous.

(a)

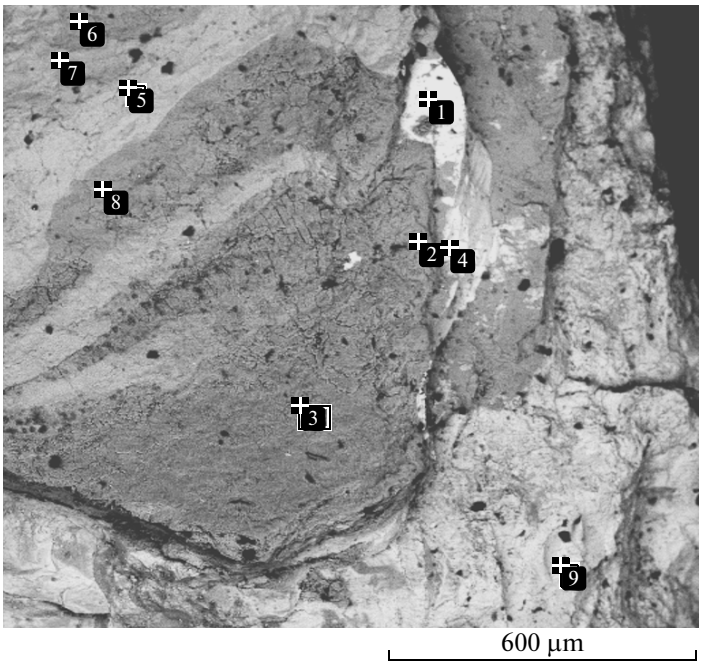

	O	Al	Si	P	S	Fe	Ni
1	8.43	0.74	1.06	13.75	0.00	43.71	32.30
2	27.84	1.48	1.14	0.00	1.95	62.35	5.24
3	47.39	0.00	0.27	0.44	1.93	45.33	4.62
4	3.62	1.29	0.00	0.57	0.00	90.14	4.38
5	21.66	0.29	0.44	0.00	0.78	74.91	1.92
6	40.09	0.33	0.49	0.49	2.38	49.25	6.97
7	39.78	0.00	0.27	0.00	1.68	53.66	4.61
8	38.96	0.28	0.42	0.00	2.26	49.94	7.15
9	8.99	0.40	0.24	0.00	31.27	59.10	0.00

(b)

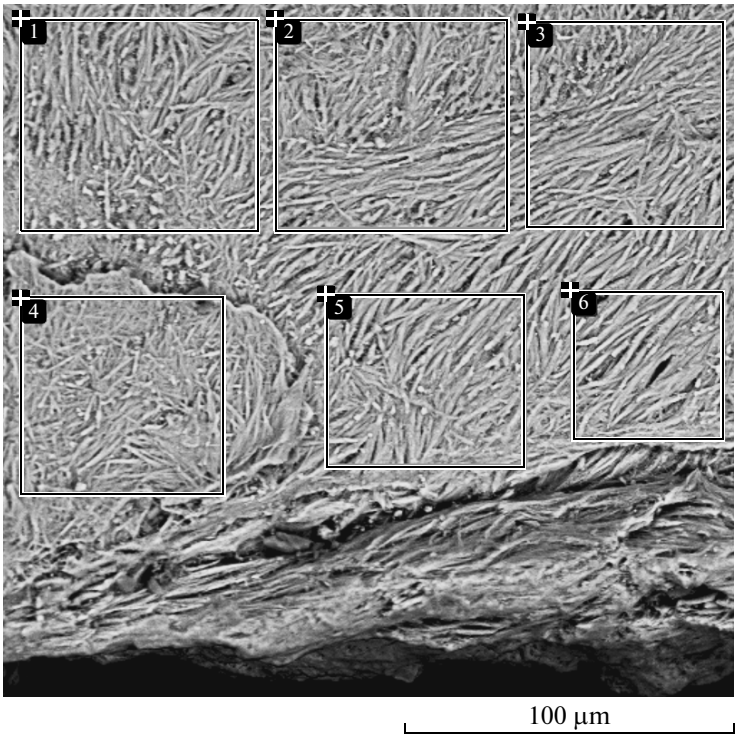

	O	S	Fe	Ni
1	38.76	2.25	55.96	3.04
2	41.06	2.57	53.90	2.47
3	40.01	2.12	54.84	3.04
4	38.27	2.06	56.56	3.11
5	39.30	2.39	55.24	3.06
6	40.11	2.07	55.36	2.46

Fig. 7. The examples of Fe-oxide with an admixture of sulfur and nickel (the Krasnoyarsk meteorite, sample gr7375sh): (a) the crust on kamacite (2, 3, 6–8) (dark gray). The process of kamacite reworking is visible: the white areas correspond to the remains of kamacite (4) and the light-gray bands mark the oxidized kamacite (5). (1) schreibersite inclusion; (9) troilite; (b) thin filaments.

Fe-sulfides, mainly troilite as well as pyrrhotite and pentlandite, are revealed by MPA in about 30% of the samples. These minerals are abundant in all stony meteorites while almost absent in iron and stony-iron meteorites (single grains are only detected in one iron meteorite, Sikhote-Alin, and in one stony-iron meteorite, Krasnoyarsk). Pyrrhotite is identified by MPA in a series of the samples; however, in none of the mete-

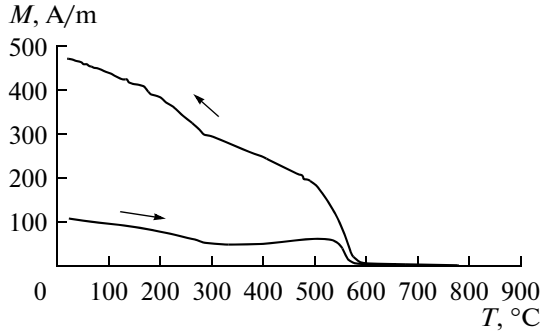

Fig. 8. The $M(T)$ curves for the sample gr7375sh (Krasnoyarsk meteorite); heating–cooling cycle.

orites has it been detected by TMA. This is probably due to the fact that pyrrhotite in the samples is high-temperature hexagonal; i.e., it is a low-magnetic antiferromagnetic; besides, it frequently occurs in the form of single grains.

Magnetite. Substantial concentrations of magnetite were revealed by TMA in many samples. To all appearances, it is a product of the secondary oxidation of kamacite and other magnetic minerals. Just as other iron oxides (hematite, goethite, etc.), magnetite has nothing in common with the preterrestrial history of a meteorite and is of no interest for the present study; it distorts the pattern of primary magnetic minerals.

The remaining minerals identified in the studied meteorites (ferrospinels, ilmenite, corundum, daubreelite, Fe-Al alloy, cinnabar, etc., see *Supplement*) are exotic and do not regularly occur in meteorites.

The Results of Studying the Tektites

All three studied tektites (moldavite 7601 and indochinites 7604 and 7605, see Table 1 and *Supplement*) are glasses compositionally close to aluminosilicates. According to MPA, the average composition of moldavite (7601) is 54% O; 5.1% Al; 35.4% Si; 2.7% K; 2% Ca; and 1% Mg ($n = 4$). The indochinite samples form two groups in terms of silica content: one with an average composition of 45.5% O; 6.3% Al; 37.2 Si; 2.5% K; 1.2% Ca; 5% Fe; 1% Mg; and 0.8% Na ($n = 5$); and another with an average composition of 54.7% O; 6% Al; 31.7% Si; 1.6% K; 0.8% Ca; 2.6% Fe; 1.4% Mg; and 1.1% Na; ($n = 8$). In contrast to moldavite, indochinites contain iron and sodium. Besides, tektite 7605 contains some minor titanium. Ore grains are not found in tektites by MPA.

According to their magnetic parameters (M_s = 0.026 (sample 7601), 0.017 (sample 7604-1) and 0.386 (sample 7604-2), 0.047 and 0.074 Am^2/kg (7605); $M_{rs}/M_s = 0.12$; $H_{cr} = 25.5$ mT (sample 7601)), the studied tektites contain minor amounts of magnetic minerals, which are close to the pseudo-single-domain (PSD) state and their grains are noticeably smaller than the diameter of the probe. Upon heating, coercivity changes insignificantly ($H_{crt}/H_{cr} = 1.08$), whereas magnetization drops severalfold, perhaps due to the oxidation (breakdown) of magnetite. $T_c = 580$°C (magnetite) is present in the $M(T)$ curve. The value of M_s suggests that the magnetite concentration in different samples ranges from 0.02 to 0.08. Sample 7604-2 with a higher magnetization contains kamacite with $T_c = 745$°C (which provides 90% M_s) and magnetite with $T_c = 580$°C (10% M_s); therefore, concentrations of kamacite and magnetite are 0.16% and 0.04%, respectively. According to T_c, kamacite contains 6% Ni. Sample 7605 shows an almost purely hyperbolic $M(T)$ curve (*Supplement*), which indicates a clearly predominant paramagnetic material. Magnetic phases with $T_c = 500$°C and $T_c = 720$°C (?) are recognized against the background hyperbolic curve. Each phase contributes less than 5% to M_s; these are more likely to be titanomagnetite and kamacite. TMA and MPA suggest that the studied tektites are products of melting of the terrestrial material containing grains of extraterrestrial origin, which demonstrates their relation to the falls of the meteorites. Thus, the studied tektites are most likely impact products.

COMPARISON OF MAGNETIC MINERALOGY OF THE THREE MAIN METEORITIC TYPES

One of the most important findings of the present study is the distribution of Ni concentrations in kamacite, taenite (Fig. 9a–9c), and schreibersite (Fig. 9d). The histograms shown in Fig. 9, which are based on MPA data, suggest the following conclusions.

(1) The cases of taenite detection in the samples are almost one-sixth as numerous as kamacite detections.

(2) The meteorites show a three-modal distribution in terms of Ni content. The first group is pure iron without Ni (mode 0% Ni); the second group is kamacite with mode 5–6% Ni in iron and stony-iron meteorites (Figs. 9a and 9b) and 3% Ni in stony meteorites (Fig. 9c); the third group is taenite with mode 50% Ni in stony meteorites (Fig. 9d).

(3) The iron and stony-iron meteorites contain only single grains of Fe-Ni alloy with more than 20% Ni (taenite) (Figs. 9a and 9b); the share of taenite, which contains 39–52% Ni, in stony meteorites with mode 50%Ni substantially increases (Fig. 9c).

(4) The values corresponding to the Ni content in kamacite and taenite are separated by a significant gap, which is filled by the Ni content in schreibersite (Fig. 9d). Thus, in terms of Ni content, Fe-Ni alloys form a regular kamacite–schreibersite–taenite succession, which contains an admixture of phosphorus in its middle part. This indicates that the occurrence of these minerals in a cosmic body is a natural result of their common formation processes, which did not

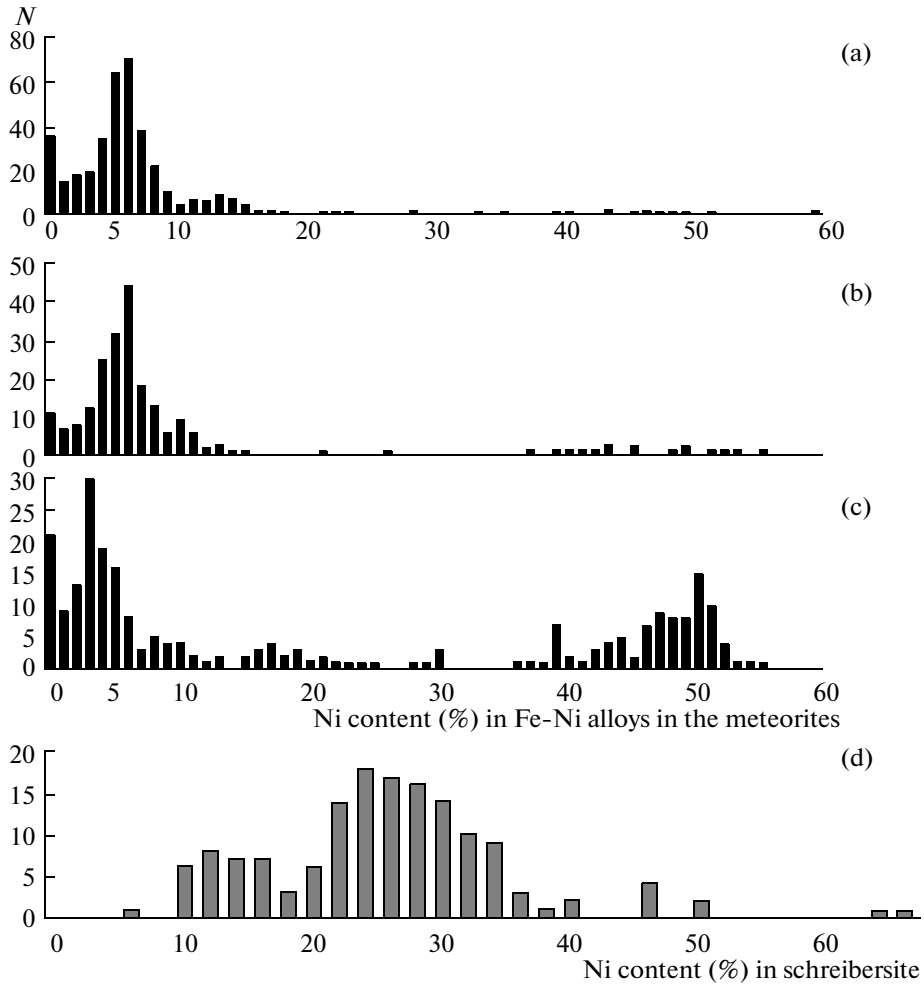

Fig. 9. The histograms of Ni content (%) in Fe-Ni alloy in various types of meteorites: (a) iron meteorites; (b) iron-stony meteorites; (c) stony meteorites; (d) the distribution of Ni content in schreibersite from iron and stony-iron meteorites. The data provided by MPA. The vertical axis measures the number of cases of Ni detection.

affect their concentrations (as mentioned above, the correlation between the contents of these minerals is absent).

The histograms in Fig. 9 are based on the MPA data alone. They reflect the number of cases of identifying grains with a given composition, but do not quantify their overall concentrations in the studied sample. Kamacite, taenite, and schreibersite concentrations estimated from a combination of TMA and MPA data (see the method) indicate that, firstly, the total average content of magnetic minerals in iron meteorites is below 70% (Table 2), which appears to be due to their substantial oxidation. Secondly, the kamacite concentration in iron meteorites is an order of magnitude higher than in stony meteorites (Table 2) while the average taenite content is uniform (within the error of determination) in all types of the meteorites (Table 2). Thirdly, the average nickel concentration in kamacite, taenite, and schreibersite slightly varies in various types of the meteorites (Table 2); i.e., different types of meteorites only differ by the concentrations of the main magnetic minerals rather than by their particular compositions. Kamacite is identified in all samples, schreibersite mainly pertains to the metallic (iron) part of the meteorites, while taenite gravitates to stony meteorites (Table 2).

The apparent contradiction with Fig. 9c is associated with the fact that Fig. 9 reflects the relative distribution of kamacite. This is also seen in the TMA data: the iron meteorites contain by a factor of 40 more kamacite than taenite, while the kamacite content in stony meteorites is only by a factor of 3.5 higher than the taenite content in this type of meteorites (Table 2).

The strikingly similar pattern of distribution of Ni content in Fe-Ni alloys from iron meteorites (Fig. 9a) and in the sediments (Fig. 1) is remarkable. Comparison of these figures shows that iron meteorites have much in common with the metallic particles from the sediments; therefore, it is reasonable to refer to the latter as micrometeorites (Grachev et al., 2009).

Table 2. Average parameters for the main types of meteorites

Characteristic	Iron	Stony-iron	Stony
Percentage of samples with kamacite, %	100	100	100
Percentage of samples with taenite, %	~50	~40	100
Percentage of samples with schreibersite, %	~50	~70	~0
Percentage of samples with Fe-sulfides, %	~2	~2	100
Kamacite content, % (scatter)	58 (18–83)	53 (20–82)	5.3 (1–7)
Taenite content, % (scatter)	1.4 (0–10)	2.7 (0–20)	1.5 (1–4)
Schreibersite content, % (scatter)	7 (0–90)	5 (0–44)	~0
Average Ni content in kamacite, %	5.9	4.6	4.6
Average Ni content in taenite, %	47	50.3	49.3
Average Ni content in schreibersite, %	26	27.8	22.3
M_s, Am^2/kg	124	123	12.5
H_{cr}, mT	15	23	49
H_{cr}/H_c	7.2	11.2	16.1
M_{rs}/M_s	0.07	0.03	0.02
T_c, °C (contribution to M_s,%)	755 (86%)	753 (87%)	756 (87%)
$T\gamma \rightarrow \alpha$, °C	642	643	640

The uniform distribution of magnetic minerals in different types of meteorites is confirmed by the similar pattern of the $M(T)$ curves (Fig. 10a). (1) All types of meteorites are clearly dominated by flat $M(T)$ curves of heating (Pechersky et al., 2011a); under the second heating, the $M(T)$ curve acquires a standard Q shape typical of ferromagnetics. (2) The Curie point of the main magnetic phase (kamacite) in the heating curve is $T_c = 740–770$°C, and the average T_c differs by 1–3°C in various types of meteorites (Fig. 10, Table 2). Kamacite contributes, on average, 86–87% to M_s. (3) In all studied samples the $M(T)$ curve of cooling records the temperature of structural transformation of taenite to kamacite (670–585°C). The average temperatures $T\gamma \rightarrow \alpha$, just as T_c, differ by 1–3°C in various types of meteorites (Table 2). The $M(T)$ curves of the Grossliebental and Egvekinot meteorites have other shapes (Fig. 10b). In addition to kamacite, these curves also record the taenite contribution. The shapes of the $M(T)$ curves for the samples containing schreibersite (sample OM-1 from the Omolon meteorite; sample gr7375 from the Krasnoyarsk meteorite; sample gr7428 from the Sao Juliao de Moreira meteorite, Fig. 10b) are also not flat in shape. The uniform pattern of TMA is violated by the processes of secondary oxidation of the meteorites, which have almost completely lost their primary magnetic minerals (Avgustinovka, Babbs Mill, sample gr7369 from Bishtyube meteorite, Zabrod'e, Cossby's Creek, Santa Catarina, (*Supplement*) and examples in Fig. 10c).

The magnetic hardness (remanent coercive force, H_{cr}) consistently increases from iron to stony meteorites, probably reflecting the more significant contribution of highly coercive tetrataenite in stony meteorites. This assumption is supported by the examples of Grossliebental, Hessle, and Egvekinot meteorites, in which the high background $H_{cr} = 50–80$ mT decreases by a factor of three to five after heating the sample to 800°C. Figure 11 shows the coercivity tending to decrease (relative to its initial value) with increasing H_{crt}. It also reflects the presence of tetrataenite, which converts to taenite when heated. This dependency is masked by the oxidation of magnetic minerals, which causes the coercivity to increase.

We note that the ratios H_{cr}/H_c and M_{rs}/M_s cited in Table 2 in all cases relate to the single-domain state of the minerals.

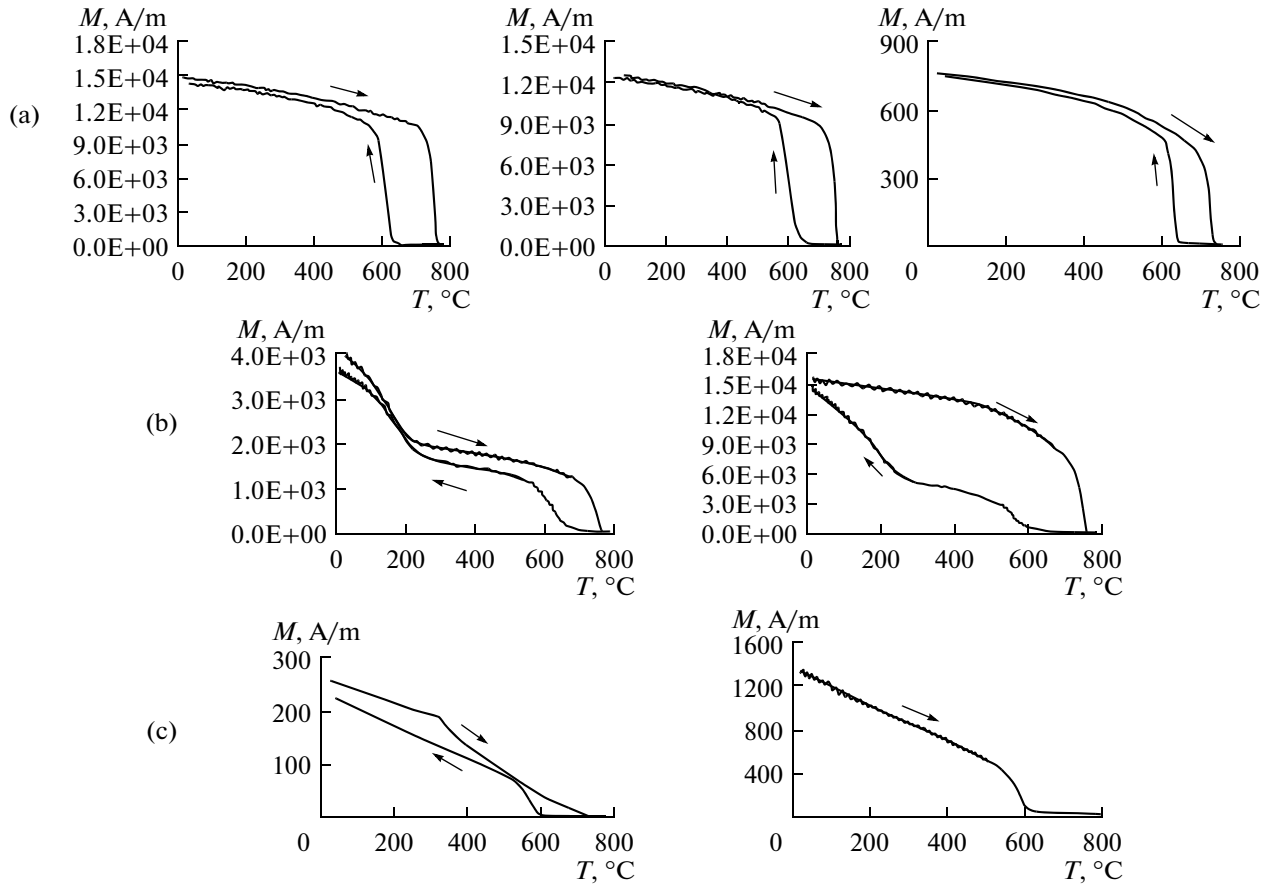

Fig. 10. The examples of $M(T)$ curves for the main types of meteorites (the heating-cooling cycle): (a) the $M(T)$ curves typical of the most meteorites. The left panel: iron meteorites; the central panel: stony-iron meteorites; the right panel: stony meteorites. (b) the $M(T)$ curves untypical of the meteorites. The left panel: the Omolon meteorite with a substantial contribution of schreibersite; the right panel: the Okhotsk meteorite wit an increased taenite percentage compared to other meteorites. (c) The $M(T)$ curves for strongly oxidized meteorites. The left panel: the Avgustinovka meteorite with kamacite; secondary magnetite, which became oxidized to hematite during heating, prevails. The right panel: the Cosby's Creek meteorite; the entire primary material is oxidized, only secondary magnetite is present.

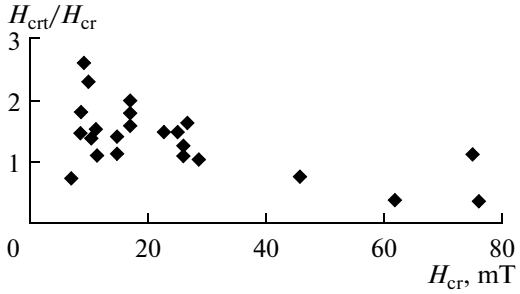

Fig. 11. The dependence of H_{crt}/H_{cr} on H_{cr}.

CONCLUSIONS

1. The combined TMA and MPA study shows that, irrespective of their type, meteorites have an identical magnetic mineral composition. The only varying parameter is the concentration of the same magnetic minerals, which increases (on average, by an order of magnitude) from stony to iron meteorites. The uniformity of magnetic minerals indicates that they were formed under similar conditions (primarily, redox conditions), despite the great diversity of the types of the meteorites containing these minerals.

2. Kamacite with a minor amount of nickel (mode 6% in iron meteorites and mode 3% in stony meteorites) is the main magnetic mineral in the studied meteorites; schreibersite and taenite are also identified. In terms of Ni content, these three minerals form a natural triad of kamacite (0–9% with average 5% Ni), schreibersite (10–34% with average 27% Ni), and taenite (38–53% with average 51% Ni). Schreibersite distinctly gravitates to Fe-Ni alloy: it is present in the iron and stony-iron meteorites and almost absent in the stony meteorites. The average taenite content is almost similar in all meteorite types. The relative taenite concentration in the iron meteorites is one-fortieth the kamacite concentration whereas the relative fraction of kamacite in the stony meteorites is only by a factor of 3.5 less than the relative concentration of

kamacite, because taenite tends to occur in stony meteorites.

3. All types of the meteorites have similar thermomagnetic $M(T)$ curves. Deviations from the common pattern are primarily due to the secondary alteration of the meteorites upon their entering into the terrestrial atmosphere and during their stay on the Earth's surface.

4. The terrestrial, lunar, and Martian basalts (crustal rocks) typically contain titanomagnetites and ferrospinels; however, most important, they are free of Fe-Ni alloys and schreibersite. The stony meteorites that contain minerals of the magnetite group but neither Fe-Ni alloys nor schreibersite are likely to have a crustal origin. We note that, in contrast to the uniform composition of the main magnetic minerals in the meteorites, the composition of titanomagnetites, which are the main magnetic minerals of the terrestrial, lunar, and Martian crusts, widely varies primarily depending on the T-fO_2 conditions. For example, the rift basalts in the continents and oceans, where these conditions are uniform, contain titanomagnetite with 12–14% Ti, whereas the volcanics from the island arcs, where the redox conditions are very diverse, the titanomagnetite composition ranges from typical rift varieties to close to magnetite. A similar situation is also characteristic of the Martian basalts. The lunar basalts are dominated by ulvospinels and other ferrospinels, which only contain Fe^{2+} and are crystallized in strongly reducing conditions.

5. The following scheme can be suggested for the planetary cross sections. The crust is dominated by the minerals of magnetite group, i.e., titanomagnetites; the upper mantle does not contain crustal magnetic minerals; as the core is approached, Fe-sulfides, Fe-Ni alloys, and schreibersite, whose formation requires iron, nickel, phosphorus, and sulfur, occur in the mantle. Judging by the distribution of schreibersite and other sulfides, sulfur is mainly concentrated in the lower mantle, whereas phosphorus tends to occur in the core. The concentration of the magnetic minerals, primarily kamacite and schreibersite, increases up to their almost 100% predominance in the core.

6. Uniform composition of the magnetic minerals of the studied meteorites indicates that they were formed under identical conditions, i.e. the formation of the planets followed a common scenario. This conclusion agrees with the concepts concerning the origin of the early Solar System (Zharkov, 1983; Hubbard, 1984; Marakushev et al., 1992; McFadden, Weissman, and Johnson, 2007; etc.). The common scenario of formation is primarily reflected in the fact that the cores of giant planets, the Earth, and the meteorites have uniform chemical composition and the members of the Solar System have similar ages. For example, solar photosphere and chondrites have almost similar chemical compositions, except for hydrogen and helium.

The Earth's core and the crust make up 12.6 and 1.4% of the total volume of the Earth; the relative volumes of the meteorites are 1.5% for iron meteorites (the core) and 1.4% for stony iron meteorites (lunar and Martian). This means that the core of the planets (iron meteorites) occupies an order of magnitude smaller volume than the Earth's core. One might suppose that the relative volume of the core of the destroyed planets (or a single planet) might have been an order of magnitude smaller than that of the Earth's core. This does not contradict the estimated percentage of native iron in the composition of the Earth, Mars, and the meteorites from the asteroid belt (Hubbard, 1984) and, apparently, corresponds to the fraction of native iron in the destroyed planets (planet), which form the asteroid belt. The small volume of crustal material compared to the remaining parts of the planets accounts for rare occurrences of the core rocks in the meteorites and, in particular, for their absence among the studied meteorites.

The uniform composition of the metallic phase is quite natural in the early Solar system. On the later stages, despite the processes of differentiation, etc., the metallic phases of all shells of the planets are similar in terms of the percentage of Ni and other impurities.

On the example of crustal situation, we observe broad variations in the compositions of the magnetic minerals, which reflect significant changes in the physicochemical conditions and, primarily, the T-fO2 regime of their crystallization. Accordingly, their uniform metallic phases suggest that the changes in the redox conditions in the melt during the crystallization of iron at this stage of planetary formation also were insignificant. This is partially due to the fact that the gravitational differentiation, at which light elements rise while heavy elements sink, should not affect metals such as nickel (which is close to the main component, iron). We note that the compositional uniformity of the magnetic minerals is globally reflected in the similarity of the histograms of nickel content (in their kamacite parts), and, mainly, in the average values of the nickel content; the fluctuations of the individual estimates, which are most prominent in schreibersite, apparently reflect local features in the formation of planetary material.

The meteorites and the Earth being of a similar age (of 4.55 ± 0.07 Ga) was noted by Patterson as early as 1956 (Patterson, 1956). The later datings of various meteorites insignificantly differ from the age estimated by Patterson and the commonly adopted age of the Solar System at 4567 Ma (*Encyclopedia ...*; McFadden, Weissman, and Johnson, 2007; Baker et al., 2005; Bonvier and Wadhwa, 2010; etc.). The younger age of the meteorites is believed to be associated with superimposed processes such as hydration, oxidation, and impact metamorphosis.

7. The similar shapes of the histograms reflecting the distribution of Ni percentage in the Fe-Ni alloy from iron meteorites and in the metallic particles from

sediments points to a common source of iron meteorites and kamacite in the cosmic dust. The degree of fragmentation of the primary material from the parent body (a planet) is the only difference. Therefore, it is reasonable to refer to the metallic magnetic particles from the sediments as the micrometeorites.

ACKNOWLEDGMENTS

We are grateful to M.N. Kandinov and A.A. Plyashkevich for providing the collections of meteoritic samples and their discussions of the results.We also thank M.L. Gelman for his reading the manuscript, valuable comments, and helpful suggestions.

REFERENCES

Baker, J., Bizzarro, M., Witting, N., Connelly, J., and Haack, H., Early Planetesimal Melting from an Age 4.566 Gyr for Differentiated Meteorites, *Nature*, 2005, vol. 436, no. 7054, pp. 1127–1131.

Bonvier, A. and Wadhwa, M., The Age of the Solar System Redefined by the Oldest Pb-Pb Age of Meteoritic Inclusion, *Nat. Geosci.*, 2010, vol. 3, pp. 637–641.

Bozorth, R., *Ferromagnetism*, Princeton, New Jersey: Van Nostrand, 1951.

Cassiamani, G., Kayzre, J.D., Ferro, R., Klotz, U.E., Locaze, J., and Wollants, P., Critical Evaluation of the Fe-Ni, Fe-Ti, and Fe-Ni-Ti Alloy Systems, *Intermetallic*, 2006, vol. 14, pp. 1312–1325.

Encyclopedia Britannica, Meteorites, Second edition. http://www.eb.com.

Frondel, J.W., *Lunar Mineralogy*, Cambridge, MA: Harvard University Press, 1975.

Gambino, R.J., McGuire, T.R., and Nakamura, Y.. Magnetic Properties of the Iron-Group Metal Phosphides, *J. Appl. Phys.*, 1967, vol. 38, no. 3, pp. 1253–1255.

Grachev, A.F., Kollmann, H.A., Korchagin, O.A., et al., The K/T boundary of Gams (Eastern Alps, Austria) and the Nature of Terminal Cretaceous Mass Extinction, Grachev, A.F., Ed., *Abh. Geol. Bundesans. (Austria)*, 2009, vol. 63, pp. 89–134.

Gus'kova, E.G., *Magnitnye svoistva meteoritov* (Magnetic Properties of Meteorites), Leningrad: Nauka, 1972.

Hubbard, W., *Planetary Interiors*, New York: Van Nostrand Reinhold, 1984.

Kohout, T., Physical Properties of Meteorites and Their Role in Planetology, *Rep. Ser. Geophys.*, 2009, no. 60, pp. 3–51.

Marakushev, A.A., Granovskii, L.B., Zinov'eva, N.G., and Mitreikina, O.B., *Kosmicheskaya petrologiya* (Space Petrology), Moscow: MGU, 1992.

McFadden, L., Weissman, P.R., and Johnson, T.V., *Encyclopedia of the Solar System*, San Diego: Academic Press, 2007.

Meteoritical Bulletin, 2000, no. 84–2010, no. 98.

Meyer, A.J.P. and Cadevill, M.C., Magnetic Properties of the Fe-Ni Phosphides, *Proc. Int. Conf. Mag. Cryst., 1961*, Supplement B-1 to *J. Phys. Soc. Japan*, 1962, vol. 17, pp. 223–225.

Nagata, T., *Rock Magnetism*, Tokyo: Maruzen, 1961.

Nagata, T., Funaki, M. and J. Danon, Magnetic Properties of Tetrataenite-Rich Iron Meteorites, *Mem. Natl. Inst. Polar Res., Spec. Issue*, 1986, vol. 41, pp. 364–370.

Nagata, T., Danon, J., and Funaki, M., Magnetic Properties of Ni-Rich Iron Meteorites, *Mem. Natl. Inst. Polar Res., Spec. Issue*, 1987, vol. 46, pp. 263–282.

Patterson, C., Age of Meteorites and the Earth, *Geochim. Cosmochim. Acta*, 1956, vol. 10, pp. 230–237.

Pechersky, D.M., Bagin, V.I., Brodskaya, S.Yu., and Sharonova, Z.V., *Magnetizm i usloviya obrazovaniya izverzhennykh gornykh porod* (Magnetism and Formation Conditions of Igneous Rocks), Leningrad: Nauka, 1975.

Pechersky, D.M. and Didenko, A.N., *Paleoaziatskii okean: petromagnitnaya i paleomagnitnaya informatsiya o ego litosfere* (Paleo-Asian Ocean: Rock Magnetic and Paleomagnetic Information on Its Lithosphere), Moscow: OIFZ RAN, 1995.

Pechersky, D.M., Nourgaliev, D.K., and Trubikhin, V.M., Native Iron in Miocene Sediments, *Rus. J. Earth Sci.*, 2008, vol. 10, ES6004. doi: 10.2205/2008ES000306

Pechersky, D.M., Metallic Iron and Nickel in Cretaceous and Cenozoic Sediments: the Results of Thermomagnetic Analysis, *J. Environ. Prot.*, 2010, vol. 1, no. 2, pp. 143–154.

Pechersky, D.M., Nurgaliev, D.K., Fomin, V.A., Sharonova, Z.V., and Gil'manova, D.M., Extraterrestrial Iron in the Cretaceous–Danian Sediments, *Izv. Phys. Earth*, 2011b, vol. 47, no. 5, pp. 379–401.

Pechersky, D.M. and Sharonova, Z.V., Thermomagnetic Evidence of Native Iron in Sediments, *Izv. Phys. Earth,* 2012, vol. 48, no. 4, pp. 320–325.

Petromagnitnaya model' litosfery (Petromagnetic Model of Lithosphere), Pashkevich, I.K. and Pecherskii, D.M., Eds., Kiev: Naukova Dumka, 1994.

Rochette, P., Weiss, B.P., and Gattacceca, J., Magnetism of Extraterrestrial Materials, *Elements*, 2009, vol. 5, pp. 223–228.

Sugiura, N. and Strangway, D.W., The Magnetic Properties of the Abee Meteorite: Evidence for a Strong Magnetic Field in the Early Solar System, *Proc. Lunar Planet. Sci.*, 1981, vol. 128, pp. 1243–1256.

Sugiura, N. and Strangway, D.W., Magnetic Studies of Meteorites, in *Meteorites and the Early Solar System II*, Lauretta D.S. and McSween, H.Y., Eds., Arizona: Univ. Arizona Press, 1987, pp.595–615.

Supplement, http://paleomag.ifz.ru/books/2012-pechersky-et-al-meteorite-data-supplement.rar

Terho, M., Pesonen, L.J., Kukkonen, I.T., and Bukovanska, M., The Petrophysical Classification of Meteorites, *Stud. Geophys. Geod.*, 1993, vol. 37, pp. 65–82.

Uehara, M. and Naramura, N., Experimental Constraints on Magnetic Stability of Chondrites and Paleomagnetic Significance of Dusty Olivines, *Earth Planet. Sci. Lett.*, 2006, vol. 250, pp. 292–305.

Wasilewski, P., Magnetic Characterization of the New Magnetic Mineral Tetrataenite and Its Contrast with Isochemical Taenite, *Phys. Earth Planet. Inter.*, 1988, vol. 52, pp. 150–158.

Weiss, B.P., Gattacceca, J., Stanley, S., Rochette, P., and Christensen, U.R., Paleomagnetic Records of Meteorites and Early Planetesimal Differentiation, *Space Sci. Rev.*, 2010, vol. 154, nos. 1–4, pp. 341–390. doi: 10.1007/s11214-009-9580-z

Zharkov, V.N., *Vnutrennee stroenie Zemli i planet* (Internal Structure of Earth and Planets), Moscow: Nauka, 1983.